



# Investigations on dielectric properties of polymer nanocomposites of PANI/Fe<sub>2</sub>O<sub>3</sub>

BHARATI BASAVARAJ\* and BASAVARAJA SANNAKKI

Department of Physics, Gulbarga University, Kalaburagi 585106, India

\*Author for correspondence (bharatipatil812@gmail.com)

MS received 13 October 2020; accepted 8 March 2021

**Abstract.** Inorganic compound of iron oxide (Fe<sub>2</sub>O<sub>3</sub>) nanoparticles was combined with the conducting polymers, which provides excellent modifications in chemical and physical properties. Therefore, the nanoparticles (NPs) of Fe<sub>2</sub>O<sub>3</sub> synthesized by green combustion method, obtained iron oxide NPs of various quantity doped with polyaniline at 10, 30 and 50 wt%. Polymerization was conducted by *in situ* polymerization route with ammonium persulphate as an oxidizing agent in aqueous hydrochloric acid solution under constant stirring at 5°C. Characterizations of synthesized samples were carried through XRD analysis. The crystallite size 31 nm is found by using Debye–Scherrer relation, also the grain size is employed to calculate dislocation density and micro strain ( $\eta$ ) which is influenced on diffraction-line broadening. And also, dielectric properties of the synthesized samples were studied as a function of frequency that shows the improved interaction between iron oxide nanoparticles and polyaniline. These polymer nanocomposites owe potential applications to the fields of optical, electrical and shielding materials.

**Keywords.** Inorganic compound; combustion; XRD; polymer nano-composites; AC conductivity.

## 1. Introduction

The well-known trend of conducting polymers, such as aniline, pyrrole, thiophene are having promising applications. Since from few decades, polyaniline is used in various fields, such as electrochemistry, electronics, light emitting diodes, optics, electro chromic displays, electromagnetic interference shielding and energy storage method. Further, its preparation is ease, environmental stability is good, low cost, low density, improved electronic properties will give potential applications in electro catalysis, rechargeable batteries, sensors and biosensors, etc. [1–5].

The addition of transition metal oxide nanoparticles with polymers will give novel features of physical properties as well as modification in structural, chemical and optical properties significantly. Therefore, the present work thrown a light towards iron oxide nanoparticles due to its impending applications in technological importance, magnetic storage devices and ferro fluids [6–10]. As the improvement in high dielectric constant polymer nanocomposites has been a major contravention of integral capacitor technology [11]. And the polymer nanocomposites of high dielectric constant are being constantly explored by the electronics industries in response to the need for power-ground decoupling to secure integrity of high-speed signals with the reduced electromagnetic interference radiated noise [12,13].

So, we have carried out synthesis of Fe<sub>2</sub>O<sub>3</sub> nanoparticles by green combustion method, then, nanoparticles of ferric oxide imparted with conducting polymer, such as polyaniline by chemical oxidative route with different weight percentages of iron oxide nanoparticles [14].

Further, the synthesized samples were characterized using XRD analysis. The dielectric measurements as frequency-dependent were carried out at room temperature for samples of PANI and PANI/Fe<sub>2</sub>O<sub>3</sub> nanocomposites at various contents, such as 10, 30 and 50% of Fe<sub>2</sub>O<sub>3</sub> nanoparticles.

## 2. Experimental

### 2.1 Materials and methods

Analytical grade monomer aniline, ammonium persulphate, iron nitrate, acetone, distilled water, filter papers and aloe vera leaves were taken.

### 2.2 Preparation of aloe vera solution

Freshly collected leaves of aloe vera plant were initially washed multiple times by distilled water before taking out the gel. It is collected in beaker then, again mixed with

distilled water in the ratio of 1:2 then, it is kept on magnetic stirrer to get homogeneous solution. Afterwards, it is filtered using Whatman No. 1 filter paper. The filtrate solution was collected in a closed container and stored in a refrigerator at 4°C for further use [15].

### 2.3 Preparation of Fe<sub>2</sub>O<sub>3</sub> nanoparticles by green synthesis method

Nanoparticles of ferric oxide were prepared by ‘self-propagating low temperature combustion method’, employing iron nitrate (Fe(NO<sub>3</sub>)<sub>2</sub>·6H<sub>2</sub>O) as a precursor and aloe vera gel solution as a fuel. Iron nitrate substance of 2.14 g was taken in a 300 ml beaker and aloe vera gel extract of 10 ml was added and both were mixed together. Thus, obtained solution was kept for stirring vigorously for a period of 40 min. The uniform mixture of both iron nitrate and fuel kept at 450°C in pre-heated muffle furnace. The mixture boils and evaporates to yield a final product of iron nanoparticles with red colour [15–17].

### 2.4 Synthesis of PANI/Fe<sub>2</sub>O<sub>3</sub> nanocomposites

The aniline monomer of 0.2 M was dissolved in de-ionized water of 100 ml. The hydrochloric acid (HCl) solution of 0.2 M was added to the aniline solution in the ratio of 1:1, resulting in aniline hydrochloride. The chemical solution was taken in a beaker and placed on the magnetic stirrer and 0.4 M of ammonium peroxy disulphate (oxidizing agent) solution in the ratio of 1:2 was added dropwise to the solution. The solution colour changes to green within few minutes. The chemical fusion was stirred continuously for 5 h at a temperature of 5°C and allowed to polymerize. After 24 h, the precipitate was collected on Whatman filter paper, the filtrate so obtained was then, washed out using acetone three to four times to absorb the water molecules and for elimination of some of the residual organic impurities. The precipitate was initially dried in an open-air atmosphere for 2 h at room temperature and then, kept in hot air oven at 70°C for 12 h and lastly gets a yield product of PANI. Further PANI/Fe<sub>2</sub>O<sub>3</sub> nanocomposites were synthesized by using the same procedure as explained in PANI synthesis. The Fe<sub>2</sub>O<sub>3</sub> NPs of 10 wt% concentration were supplementary before adding oxidizing agent as ammonium peroxy disulphate to the aniline solution. A similar procedure is used for the synthesis of other different weight percentages of polymer nanocomposites, such as 10, 30 and 50 wt%. The prepared samples were used for characterizations. The PANI–nanocomposites powder of 350 mg was weighed using a single pan balance, for preparation of pellets by employing 3–4 tons of pressure using a pellet making machine. Further, silver paste was coated on both the surfaces of pellets for providing good electrical contact between them, so that it acts like a capacitor. The prepared

pellets of PANI/Fe<sub>2</sub>O<sub>3</sub> nanocomposites were used for dielectric measurements, such as capacitance, dissipation, impedance and phase angle to study the electrical properties on frequency-dependent at room temperature using the LCR Q-meter (Keithely).

## 3. Results and discussion

### 3.1 XRD analysis

XRD analysis is used to study the nature of crystallinity of the synthesized sample and for calculating the crystallite size. We have done XRD using the powder method for PANI, Fe<sub>2</sub>O<sub>3</sub> NPs and PANI/Fe<sub>2</sub>O<sub>3</sub> nanocomposites. The patterns of XRD were recorded in terms of 2θ in the range of 10–80° with a step size of 4°. Figure 1a shows the XRD pattern of PANI and its characteristic broad peak occurred at 25.50°, which evidences the amorphous behaviour of synthesized PANI [22].

Figure 1b shows the XRD pattern of Fe<sub>2</sub>O<sub>3</sub> nanoparticles, the peaks occurred at the angles of 33.25, 35.71, 43.04, 54.45, 57.04, 63 and 71.63°, are the characteristic peaks of Fe<sub>2</sub>O<sub>3</sub> NPs which are highly intense. The sharp peaks of XRD, clearly infer the crystalline nature of nanocomposites. The (hkl) values of the planes are (014), (110), (113), (116), (018), (214) and (101) for the prepared nanoparticles of Fe<sub>2</sub>O<sub>3</sub> [18]. The crystallite size of 31 nm is calculated by using Debye–Scherrer formula (1) data given in table 1.

$$D = \frac{k\lambda}{\beta \cos \theta} \quad (1)$$

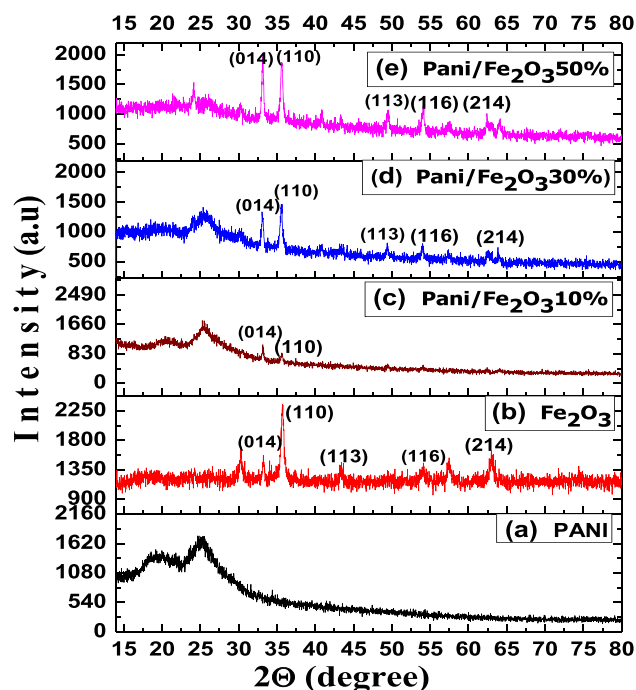


**Figure 1.** X-ray diffraction patterns for (a) PANI, (b) Fe<sub>2</sub>O<sub>3</sub> and (c, d, e) PANI/Fe<sub>2</sub>O<sub>3</sub> nanocomposites.

**Table 1.** XRD pattern analysis used to calculate crystallite size by using FWHM and  $2\theta$  values.

Peaks	(hkl) plane values	$2\theta$ (°)	FWHM ( $\beta$ )	Particle size ( $D$ ) nm
Peak 1	(104)	30.2	0.712	29.89
Peak 2	(110)	35.7	0.527	31.52
Peak 3	(116)	54.0	0.548	30.88
Peak 4	(018)	57.4	0.544	31.85
Peak 5	(214)	63.0	0.686	30.95

Figure 1c, d, e also shows the XRD peaks occurred at  $2\theta = 33.25, 35.71, 63.04, 54.04, 57.45, 63$  and  $71.63^\circ$  with the planes (014), (110), (113), (116), (018), (214) and (101) for PANI/Fe<sub>2</sub>O<sub>3</sub> nanocomposites of 10, 30 and 50 wt%. It is noteworthy that the XRD peak of PANI disappeared for higher nanocomposites structure. The shift of PANI peak in nanocomposites is observed due to the doping of Fe<sub>2</sub>O<sub>3</sub> NPs in polymer PANI which also reduce the PANI peak in nanocomposites, since it is evidenced due to the formation of nanocomposites from XRD pattern analysis [19]. The peaks grown for PANI/Fe<sub>2</sub>O<sub>3</sub> nanocomposites were similar to the Fe<sub>2</sub>O<sub>3</sub> NPs peaks confirming the type of  $\alpha$ -Fe<sub>2</sub>O<sub>3</sub> crystal structure [20]. The patterns of XRD shows the existence of two different phases i.e., PANI and Fe<sub>2</sub>O<sub>3</sub>, supporting the formation of PANI/Fe<sub>2</sub>O<sub>3</sub> nanocomposite and also it is noticed that as wt% of Fe<sub>2</sub>O<sub>3</sub> NPs increases in polyaniline, the intensity of Fe<sub>2</sub>O<sub>3</sub> NPs increases where as PANI is disappearing in 50 wt%. These characteristic peaks reveal the semi-crystalline nature of PANI/Fe<sub>2</sub>O<sub>3</sub> nanocomposites.

### 3.2 Dislocation density

The dislocation density was calculated from the grain size using the following equation:

$$\delta = 1/D^2. \tag{2}$$

The dislocation density of different wt% of polymer nanocomposites is given in table 2.

**Table 2.** The grain size and dislocation density calculated for PANI/Fe<sub>2</sub>O<sub>3</sub> nanocomposites.

wt% of material	Grain size (nm)	Dislocation density (kg m <sup>-3</sup> )
PANI/Fe <sub>2</sub> O <sub>3</sub> 10%	11.30	0.00738
PANI/Fe <sub>2</sub> O <sub>3</sub> 30%	13.16	0.00557
PANI/Fe <sub>2</sub> O <sub>3</sub> 50%	16.54	0.00382

### 3.3 Micro strain of Fe<sub>2</sub>O<sub>3</sub>

The analysis of grain size from diffraction peak width will result in the micro strain and the major parameters to influence diffraction-line broadening are particle size, micro strain and instrumental factors.

Earlier, we used proposed theory of diffraction-line broadening for a deformed metal to analyse the high-pressure data. How the line width depends on micro strain and grain size is expressed by Jing Yang *et al* [21].

$$(2\omega_{hkl} \cos \theta_{hkl})^2 = (\lambda/d)^2 + \eta_{hkl}^2 \sin^2 \theta_{hkl}, \tag{3}$$

where  $2\omega_{hkl}$  is the FWHM corrected for instrumental effects. Instrumental broadening can be measured using a stress-free sample with a known grain size, but here, instrumental broadening was corrected using the diffraction pattern of the sample under the bare minimum pressure. And in equation (3),  $\lambda$  is the wavelength of X-ray,  $\theta_{hkl}$  is the Bragg angle,  $d$  is the grain size of the crystallites and  $\eta_{hkl}$  is the micro strain.

The plot drawn with  $(2\omega_{hkl} \cos \theta_{hkl})^2$  vs.  $\sin^2 \theta_{hkl}$  which is the micro strain ( $\eta$ ). Also, by using the intercept value from the plotted graph, we can confirm wavelength ( $\lambda$ ) and crystallite size ( $d$ ). Figure 2 shows the typical plots which can be fitted with a linear function. The diffraction-line patterns from the samples reveal broadening under non-hydrostatic compression. The line widths are calculated by plotting  $(2\omega_{hkl} \cos \theta_{hkl})^2$  vs.  $\sin^2 \theta_{hkl}$ .

Material	Intercept (c)	Micro strain ( $\eta$ ) (slope)
Fe <sub>2</sub> O <sub>3</sub>	0.32232	0.01317

## 4. Dielectric properties

### 4.1 Dielectric constant

Dielectric constant and dielectric loss as functions of frequency for PANI and nanocomposites were studied at room temperature. The measured values of capacitance for PANI and PANI/Fe<sub>2</sub>O<sub>3</sub> nanocomposites of 10, 30, 50 wt% were used to find dielectric parameters by using equation (4).

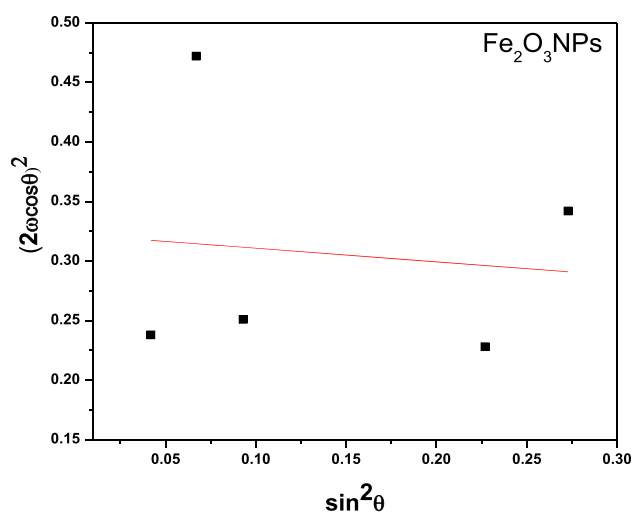
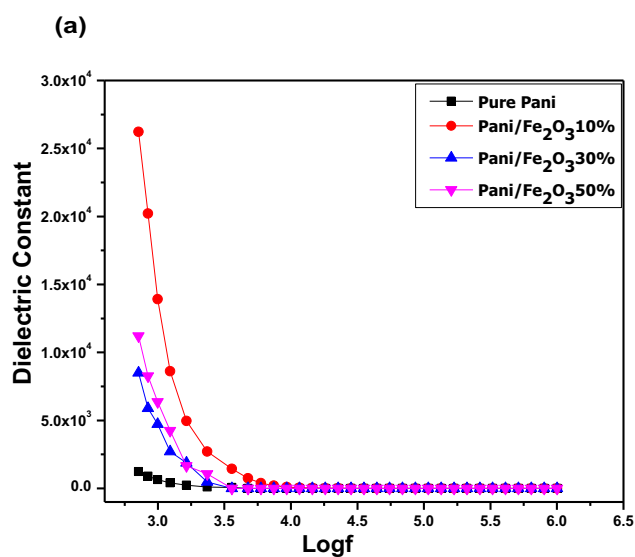


**Figure 2.** Variation of  $(2\omega_{hkl} \cos \theta_{hkl})^2$  vs.  $\sin^2 \theta_{hkl}$  for  $\text{Fe}_2\text{O}_3$  nanoparticles.

$$\varepsilon' = \frac{cd}{\varepsilon_0 A} \quad (4)$$

The variation of dielectric constant with frequency is shown in figure 3a ranging from 50 Hz–35 MHz. The dielectric constants of PANI and polymer nanocomposites of 10, 30, 50 wt% decreased as frequency increased up to 3.5 MHz. The decrease in dielectric constant due to the presence of hydrogen atoms in the polymer in a highly reduced state, reveals that polarization dielectric might have been lost. These hydrogen atoms could participate in the partial reduction of  $\text{Fe}^{3+}$  ions of  $\text{Fe}_2\text{O}_3$  particles consequently, reduction of  $\text{Fe}^{3+}$  ions might have increased at a higher frequency, which would also contribute to a decrease in dielectric constant [22].



Further, for higher frequency region, dielectric constant remains almost constant, it depicts independent of frequency because of electrical relaxation process. It is also noticed that for PANI/ $\text{Fe}_2\text{O}_3$  nanocomposite at 10 wt%, the dielectric constant is very high as compared to PANI and other nanocomposites, this is due to electric dipoles which have sufficient time to align with the field before the field changes its direction. This type of very high increase in dielectric constant could be attributed to high packing density of iron oxide NPs in polyaniline matrix [23]. The shorter time available for the dipoles to align because of which dielectric constant decreases [24] and the dielectric loss  $\varepsilon''$  decreases due to the migration of ions in the material. And the minimum values of the dielectric losses suggest PANI/ $\text{Fe}_2\text{O}_3$  nanocomposite to be good shielding material [25].

#### 4.2 AC conductivity

AC conductivity is studied as dependence of frequency for polyaniline and PANI/ $\text{Fe}_2\text{O}_3$  nanocomposites of various weight percentages at room temperature and is determined by using the dielectric data employing the following equation (5).

$$\sigma_{AC} = \varepsilon' \varepsilon_0 \omega \tan \delta. \quad (5)$$

Figure 3b shows the electrical conductivity of pure PANI and 10, 30, 50 wt% of  $\text{Fe}_2\text{O}_3$  in polymer nanocomposites. It is observed that the AC conductivity ( $\sigma_{AC}$ ) remains constant up to 5.75 MHz subsequently, it increased for higher frequencies and it also increases with increasing  $\text{Fe}_2\text{O}_3$  NPs content in PANI matrix. And the increase in conductivity with  $\text{Fe}_2\text{O}_3$  contents could be attributed due to alignment and straightening of PANI chains on the surface of  $\text{Fe}_2\text{O}_3$  particles [26].

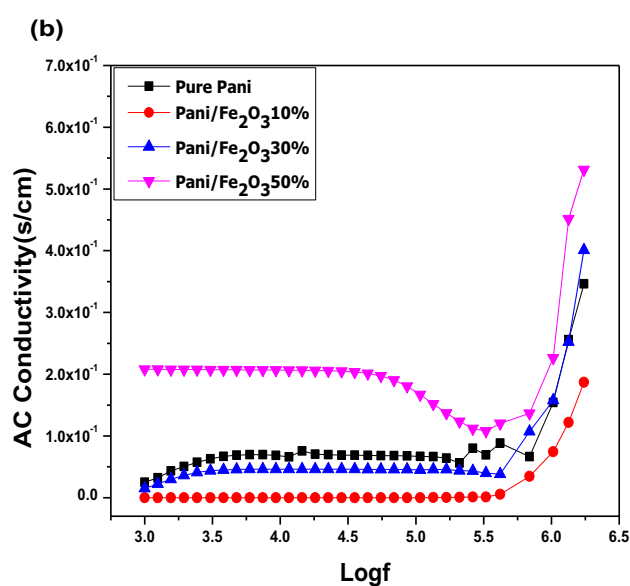


**Figure 3.** Variations in (a) dielectric constant and (b) AC conductivity with frequency for PANI and PANI/ $\text{Fe}_2\text{O}_3$  nanocomposites.

At 50 wt% nanocomposite shows linear increase in the AC conductivity. This may be due to greater freedom of movement in the dipole molecular chains within the polyaniline at higher frequencies. Because of dipole polarization, 10 and 30 wt% of PANI/Fe<sub>2</sub>O<sub>3</sub> nanocomposites' conductivity value is low. These actions of the nanocomposites may be due to the variation in the dispersion of iron oxide nanoparticles in PANI matrix.

## 5. Conclusions

The nanoparticles of iron oxide were synthesized by green route; further, the NPs were added to polyaniline by *in situ* polymerization method successfully. The samples were characterized by using XRD and electrical properties. The XRD patterns analysis depicted the presence of two different phases of PANI and Fe<sub>2</sub>O<sub>3</sub>, supporting the formation of PANI/Fe<sub>2</sub>O<sub>3</sub> nanocomposites and the size of crystallite for Fe<sub>2</sub>O<sub>3</sub> NPs found to be 31 nm range which is also used to calculate the dislocation density, micro strain ( $\eta$ ) of different wt% of NCPs to analyse the grain size from diffraction peak width will result in the micro strain and the major parameters to influence diffraction-line broadening are particle size and micro strain. The electrical conductivity influences due to the presence of iron oxide nanoparticles in the polyaniline matrix. And further, it is observed that the dielectric constant is high for 30 wt% of PANI/Fe<sub>2</sub>O<sub>3</sub> with low dielectric loss. Because of conductivity, these nanocomposites may find potential application in microwave frequencies as absorbing and shielding materials.

## Acknowledgements

We are grateful to the Department of Physics and Material Science at GUK, for providing necessary characterization facilities.

## References

- [1] Chandrakanthi R L N and Careem M A 2002 *Thin Solid Films* **417** 51
- [2] Somani P R, Marimuthu R, Mulik U P, Mulik S R, Sanikar S R and Amalnerkar D 1999 *Synth. Met.* **106** 45
- [3] He Y 2005 *J. Mater. Chem. Phys.* **268** 134
- [4] Geng L, Zhao Y, Huang X, Wang S, Zhang S and Wu J 2007 *Sens. Actuators* **34** 568
- [5] Yu S, Xi M, Jin X, Han K, Wang Z and Zhu H 2010 *J. Catal. Commun.* **57** 1125
- [6] Buron C C, Lakard B, Monnin A F, Moutarlier V and Lakard S 2011 *Synth. Met.* **161** 2162
- [7] Adhikari B and Majumdar S 2004 *Prog. Polym. Sci.* **29** 699
- [8] McQuade D T, Pullen A E and Swager T M 2000 *Chem. Rev.* **100** 2537
- [9] Gerard M, Chaubey A and Malhotra B D 2002 *Biosens. Bioelectron.* **17** 345
- [10] Chiang J P and MacDiarmid A G 1986 *Synth. Met.* **13** 193
- [11] Sugii N, Yamada H, Kagaya O, Yamasaki M, Sekine K, Yamashita K *et al* 1998 *Appl. Phys. Lett.* **72** 261
- [12] Popielarz R, Chiang C K, Nozaki R and Obrzut J 2001 *Macromolecules* **34** 5910
- [13] Koul S, Chandra R and Dhawan S K 2000 *Polymer* **41** 9305
- [14] Laberty C, Alphonse P, Demai J J, Sarada C and Rousset A 1997 *Mater. Res. Bull.* **32** 249
- [15] Bhuiyan Md S H, Yusuf Miah Md, Shujit Chandra Paul, Das Aka T, Saha O, Rahaman Md M *et al* 2020 *Heliyon* **6** e04603
- [16] Karade V C, Parit S B, Dawkar V V, Devan R S, Choudhary R J, Kedge V V *et al* 2019 *Heliyon* **5** e02044
- [17] Ahmmad B, Leonard K, Islam Md S, Kurawaki J, Muruganandham M, Ohkubo Takahiro *et al* 2013 *Adv. Powder Technol.* **24** 160
- [18] Jeong J M, Choi B G, Lee S C, Lee K G, Chang Sung-Jin, Han Young-Kyu *et al* 2013 *Adv. Mater.* <https://doi.org/10.1002/adma.201302710>
- [19] Wang S, Hu Y, Zong R, Tang Y, Chen Z and Fan W 2004 *Appl. Clay Sci.* **25** 49
- [20] Khuspe G D, Navale S T, Bandgar D K, Sakhare R D, Chougule M A and Patil V B 2014 *Electron. Mater. Lett.* **10** 191
- [21] Yang Jing, Deng Wen, Li Qiang, Li Xin, Liang Akun, Su Yuzhu *et al* 2020 *Matter Radiat. Extremes* **5** 058401
- [22] Bae W J, Jo W H and Park Y H 2003 *Synth. Met.* **132** 239
- [23] Mallikarjuna N N, Manohar S K, Kulkarni P V, Venkataraman A and Aminabhavi T M 2005 *J. Appl. Polym. Sci.* **97** 1868
- [24] Sannakki Nagaraja, Ambalagi S M, Inamdar H K, Bharathi B, Mahalesh D, Ambika Prasad M V N *et al* 2018 *J. Nanosci. Technol.* **4** 516
- [25] Singh Kuldeep, Ohlan Anil, Kotnala R K, Bakhshi A K and Dhawan S K 2008 *Mater. Chem. Phys.* **112** 651
- [26] Bashir T, Shakoor A, Ahmad E, Saeed M, Niaz N A and Tirmizi S K 2015 *Polym. Sci. Ser. B* **57** 257